Research Square

Preprints are preliminary reports that have not undergone peer review.
They should not be considered conclusive, used to inform clinical practice,
or referenced by the media as validated information.

CT-Derived Hounsfield Units Correlate with Dorr Classification and Objectively Identify Dorr Type C Morphology in MAKO-Assisted Total Hip Arthroplasty

Zubin Mathew

zamdmy@umsystem.edu

University of Missouri-Kansas City School of Medicine

Riya Mehta

University of Missouri-Kansas City School of Medicine

Firas Batrash

University of Missouri-Kansas City School of Medicine

Samir Mehta

University of Missouri-Kansas City School of Medicine

Alfred Kankam

St. Luke's Hospital

John W Krumme

University of New Mexico

Research Article

Keywords: total hip arthroplasty, Hounsfield units, Dorr classification, robotic arthroplasty, MAKO, preoperative planning

Posted Date: August 18th, 2026

DOI: https://doi.org/10.21203/rs.3.rs-10529036/v1

License: This work is licensed under a Creative Commons Attribution 4.0 International License.
Read Full License

Additional Declarations: No competing interests reported.

Abstract

Background

Radiographic Dorr classification used before total hip arthroplasty (THA) is subjective. Preoperative computed tomography (CT) scans for robotic THA allow Hounsfield unit (HU) quantification, providing an objective measure of bone quality.

Methods

We retrospectively reviewed 578 patients undergoing MAKO-assisted primary THA (2019–2024); 489 met inclusion criteria. Femoral neck HU and an average composite HU (L4, femoral neck, intertrochanteric) were compared across Dorr types. ROC and regression analyses identified thresholds predictive of high-risk Dorr Type C morphology.

Results

Femoral neck HU decreased stepwise across Dorr A (171.9), B (124.5), and C (77.9) hips ($P < 0.001$), as did average HU (186.5, 136.6, and 92.2, respectively; $P < 0.001$). Femoral neck HU predicted Dorr C morphology with an AUC of 0.81 (cutoff ≤ 87 HU; 62.4% sensitivity, 84.0% specificity). Average HU demonstrated stronger discrimination with an AUC of 0.88 (cutoff ≤ 117.6 HU; 82.2% sensitivity, 80.2% specificity). On multivariable regression adjusting for age, BMI, and sex, lower average composite HU remained independently associated with higher Dorr grade (OR 1.43 per 10 HU decrease, $P < 0.001$) and maintained strong predictive performance for Dorr C morphology (adjusted AUC 0.879).

Conclusion

CT-derived HU measurements correlate strongly and stepwise with Dorr classification. Average composite HU outperformed isolated femoral neck HU for identifying Dorr Type C morphology. A threshold of ≤ 117.6 HU serves as a robust, covariate-independent screening tool to objectify preoperative planning and guide stem selection.

Introduction

Total hip arthroplasty (THA) volumes continue to increase, and preoperative assessment of proximal femoral bone quality remains important to implant selection, fixation strategy, and complication avoidance [1, 2]. Dorr classification categorizes femoral canal morphology into Type A, B, and C based on cortical thickness and metaphyseal fit [3]. Type C femora are associated with thinner cortices, reduced metaphyseal engagement, and greater risk of periprosthetic femoral fracture with cementless fixation [3–6].

Despite widespread use, Dorr classification is derived from plain radiographs and remains inherently subjective, with moderate intra-examiner and inter-examiner reliability [3, 4, 5]. Variability in technique and classification criteria may limit its reliability in preoperative decision-making [4, 6]. Computed tomography (CT)-based Hounsfield unit (HU) quantification has emerged as a method of assessing bone mineral density [8, 9]. HU values correlate strongly with dual-energy X-ray absorptiometry (DEXA) derived bone mineral density [9–11]. Preoperative CTs are required for some robotic-arm-assisted THA, yet HU measurements are rarely reported systematically in robotic THA workflows [12–14]. Because CT is already acquired for planning, HU analysis can add objective bone-quality information without additional radiation, software, or cost [15–18].

This study determines whether Dorr morphology, which is already clinically meaningful for fixation risk, can be confirmed using objective values from CT. The purpose was to determine whether femoral neck HU and composite average HU correlate with Dorr classification, whether HU thresholds can identify Dorr Type C morphology in CT-based robotic primary THA, and whether HU can further stratify periprosthetic fracture risk within Dorr classification groups. Collectively, these findings were intended to provide surgeons with an objective, CT-focused adjunct to the classic HU to guide implant selection and strategy in primary THA.

Methods

Study Design and Setting

We retrospectively reviewed patients who underwent primary MAKO CT-planned THA within the Saint Luke's Health System (2019–2024) and were coded with CPT 27130. Procedures by three orthopaedic surgeons were included.

Participants

Eligible patients underwent MAKO-assisted primary THA with available preoperative CTs. 21 patients were excluded as X-rays could not be used to assign Dorr type, 68 patients were excluded as CT did not show all three HU measurement sites or have documented MAKO assistance. The institutional review board granted exemption status (category 4; SLHS-24-076).

Data Collection

Variables included age, sex, race, Body Mass Index (BMI) category, medical comorbidities, surgical approach, implant type, Dorr classification, femoral neck HU, and mean HU across L4 vertebral body (L4), femoral neck (FN), and intertrochanteric region (IT). Dorr type was assigned from preoperative radiographs using cortical thickness relative to canal width with the type A ratio being less than 0.5, type B being 0.5 to 0.75, and type C being above 0.75. HU values were measured in Epic software on axial CT

by placing a region of interest (ROI) at the center of L4, FN, and IT. These three values were averaged. Sites were chosen based on prior correlation with DEXA [11, 19, 20]. L4 was used because upper lumbar levels were inconsistently visible and prior work supports its use [21].

Statistical Analysis

HU was compared across Dorr types using Kruskal-Wallis and Mann-Whitney U pairwise tests. Spearman correlation assessed ordinal Dorr-HU association. Receiver Operating Characteristic (ROC) analysis treated Dorr C as the positive class. The Youden index determined optimal thresholds. Multivariable ordinal logistic regression (Dorr A-C) and binary logistic regression (C vs A/B) adjusted for age, BMI category, and sex. Continuous HU was modeled per 10-unit decrease; dichotomized predictors used ROC-derived cutoffs (FN ≤ 87 HU; average ≤ 117.6 HU). Fit was compared with pseudo R^2 and AIC; covariate-adjusted discrimination used model-predicted probabilities. Analyses were performed in Python 3.9. $P < 0.05$ was considered significant.

Results

Patient Cohort Demographics

Of 578 reviewed patients, 68 were excluded for incomplete CT ROI and 21 for missing radiographic Dorr assignment, leaving 489 patients: 171 Dorr A (35.0%), 217 Dorr B (44.4%), and 101 Dorr C (20.7%) (Table 1). Dorr C patients were older (72.0 ± 10.2 vs 67.5 ± 9.8 for Type B and 65.3 ± 11.1 for Type A), more often women (73.3% vs 46.2% for Type A), and less often obese by BMI category (26.7% vs 47.4% for Type A) (Table 1).

Table 1. Patient demographics and baseline characteristics stratified by Dorr classification

Dorr Classification	n (%)	Age years (mean ± SD)	Female, n (%)	BMI category, Obese n (%)
Type A	171 (35.0)	65.3 ± 11.1	79 (46.2)	81(47.4)
Type B	217 (44.4)	67.5 ± 9.8	121 (55.8)	70 (32.3)
Type C	101 (20.7)	72.0 ± 10.2	74 (73.3)	27 (26.7)
Overall	489 (100.0)	67.7 ± 10.6	274 (56.0)	178 (36.4)

Abbreviations: SD, Standard Deviation; n, number

Proximal Femoral Attenuation Across Dorr Classifications

CT attenuation declined linearly from Dorr A to C (Table 2, Figure 1). Mean femoral neck HU was 171.9 ± 65.5 (A), 124.5 ± 53.0 (B), and 77.9 ± 46.0 (C). Average HU across 3 sites was 186.5 ± 48.0, 136.6 ± 36.0, and 92.2 ± 35.6, respectively. All pairwise comparisons were significant ($P < 0.001$). Spearman

correlation was stronger for average HU (ρ = -0.662; *P* < 0.001) than femoral neck HU (ρ = -0.529; *P* < 0.001).

Table 2. Femoral neck and average Hounsfield units by Dorr classification

HU Measurement Site	Dorr Type A (n=171)	Dorr Type B (n=217)	Dorr Type C (n=101)	Kruskal-Wallis (*p*-value)
Femoral Neck HU				(<0.001)
Mean ± SD	171.9 ± 65.5	124.5 ± 53.0	77.9 ± 46.0	
Median (IQR)	165.0 (121.0-210)	118 (88.0-154.0)	67.7 (42.4-102.5)	
Average HU (composite)				(<0.001)
Mean ± SD	186.5 ± 48.0	136.6 ± 36.0	92.2 ± 35.6	
Median (IQR)	182.0 (151.0-218.0)	132.0 (114.0-160.0)	88.5 (70.8-111.3)	

Abbreviations: HU, Hounsfield unit; SD, standard deviation; IQR, interquartile range

Note on composite Average HU: Average HU values represent the composite regional average derived across the L4 vertebral body, femoral neck, and intertrochanteric regions.

Diagnostic Thresholds and Receiver Operating Characteristic (ROC) Curve Analysis

Average HU discriminated Dorr C (n=101) from A/B (n=388) better than femoral neck HU (AUC 0.88 vs 0.81; Table 3, Figure 2). Optimal cutoffs were ≤117.6 HU for average HU (sensitivity 82.2%, specificity 80.2%) and ≤87 HU for femoral neck HU (sensitivity 62.4%, specificity 84.0%).

Table 3. Receiver operating characteristic (ROC) analysis for prediction of Dorr Type C morphology

HU Measurement	AUC (95% CI)	Optimal Cutoff (HU)	Sensitivity (%)	Specificity (%)
Femoral Neck HU	0.81	≤ 87.0	62.4%	84.0%
Average HU (Composite)	0.88	≤ 117.6	82.2%	80.2%

Abbreviations: HU, Hounsfield unit; AUC, area under the curve; CI, confidence interval

Note on composite Average HU: Average HU values represent the composite regional average derived across the L4 vertebral body, femoral neck, and intertrochanteric regions.

Note: Analysis evaluates Dorr Type C (n = 101) as the positive class against combined Dorr Type A and B cohorts (n = 388)

Periprosthetic Fracture Event Analysis

Postoperative periprosthetic fractures (PPF) occurred in 6 patients (1.23%). All 6 PPF events occurred exclusively in patients with concordant Dorr Type C morphology and baseline Femoral Neck HU <100 (n=71, fracture incidence 8.45%, 95% CI: 3.93%–17.24%). No fractures were observed in the low-risk cohort (Dorr A/B and FN HU ≥100, n=292) or in either intermediate-risk subgroup (Dorr C with FN HU ≥100, n=30; Dorr A/B with FN HU <100, n=96).

Multivariable Regression Analysis

After adjustment for age, BMI category, and sex, lower average HU remained associated with higher Dorr grade (OR 1.43 per 10 HU decrease, 95% CI 1.35-1.51; $P < 0.001$; pseudo R^2 0.285; AIC 749; Table 4) and outperformed femoral neck HU (OR 1.20 per 10 HU decrease, 95% CI 1.16-1.25; $P < 0.001$; pseudo R^2 0.175; AIC 863; Table 4). In binary models for Dorr C, average HU again fit best (OR 1.52 per 10 HU decrease; pseudo R^2 0.351; AIC 333; 95% CI 1.38-1.67; $P < 0.001$; Table 4). Threshold models (average ≤117.6: OR 15.37; FN ≤87: OR 6.81;) showed comparable discrimination despite slightly lower fit. Female sex predicted higher Dorr grade in a covariate-only model (OR 1.87, $P < 0.001$) but not after adding average HU (OR 1.17, P = 0.45). Adjusted AUC for Dorr C was essentially unchanged compared to unadjusted HU alone (0.879 vs 0.876 for average HU).

Table 4: Model Comparison

Model	Outcome	HU predictor	Form	Adjusted for Age, BMI, sex	OR (95% CI)	Pseudo R^2	AIC
1	Ordinal Dorr (A<B<C)	Average HU	Continuous (per 10↓)	Yes	1.43 (1.35–1.51)	0.285	749
2	Ordinal Dorr (A<B<C)	Femoral neck HU	Continuous (per 10↓)	Yes	1.20 (1.16–1.25)	0.175	863
3	Dorr C vs A+B	Average HU	Continuous (per 10↓)	Yes	1.52 (1.38–1.67)	0.351	333
4	Dorr C vs A+B	Average HU	≤117.6 threshold	Yes		0.301	358
5	Dorr C vs A+B	Femoral neck HU	Continuous (per 10↓)	Yes	1.26 (1.19–1.34)	0.248	385
6	Dorr C vs A+B	Femoral neck HU	≤87 threshold	Yes		0.199	409

Abbreviations: HU, Hounsfield unit, OR, Odds Ratio; CI, Confidence Interval; Pseudo R^2, McFadden's pseudo coefficient of determination; AIC, Akaike Information Criterion; ↓ decrease.

Discussion

In this retrospective single-center study of 489 patients undergoing CT-planned MAKO-assisted primary THA, CT-derived Hounsfield units demonstrated a strong, stepwise relationship with radiographic Dorr classification. Both femoral neck and composite HU values declined significantly from Dorr Type A to Type C. However, the three-site composite measure showed the strongest correlation with Dorr grade and superior discrimination of Type C morphology. An average composite HU threshold of ≤117.6 identified Dorr Type C femurs with 82.2% sensitivity and 80.2% specificity, and its predictive performance remained essentially unchanged after adjustment for age, sex, and BMI. These findings suggest that attenuation data already available from robotic-planning CT can provide an objective, workflow-integrated adjunct to the traditionally subjective Dorr classification. Although the small number of periprosthetic fractures precludes definitive outcome-based conclusions, the observation that all six fractures occurred among patients with concordant Dorr Type C morphology and low HU further supports investigation of combined radiographic and CT-based bone-quality assessment for preoperative risk stratification and femoral fixation planning.

Relationship Between Dorr Morphology and CT Attenuation

The progressive decrease in HU from Dorr Type A through C is consistent with the structural basis of the Dorr classification. Dorr classification describes proximal femoral structure, including cortical thickness,

canal dimensions, and metaphyseal fit [3], with Type C femurs demonstrating the thinnest cortices and least favorable metaphyseal engagement [4,17]. In the present cohort, these radiographic changes were accompanied by measurable reductions in CT attenuation. Mean femoral neck HU decreased from 171.9 in Type A hips to 77.9 in Type C hips, while composite average HU decreased from 186.5 to 92.2. The significant differences among Dorr types suggest that the relationship is not limited to distinguishing the most severe Type C morphology but instead reflects a graded association between radiographic morphology and skeletal attenuation [Figure 1].

Patients with Dorr Type C morphology were older, more frequently women, and less frequently categorized as obese, findings that are consistent with established demographic patterns of declining bone quality [22]. Despite this, composite HU remained strongly associated with Dorr classification after adjustment for age, sex, and BMI. Furthermore, covariate adjustment did not meaningfully reduce discrimination for Dorr Type C (AUC 0.876 vs 0.879). These findings indicate that HU provides information beyond demographic characteristics that are commonly used as indirect proxies for bone quality. They do not, however, imply that demographic factors are clinically unimportant. Rather, direct attenuation measurements may complement demographic risk assessment when radiographic morphology is uncertain.

The present findings are consistent with prior opportunistic CT studies demonstrating relationships among HU, DEXA-derived bone mineral density, osteoporosis, and proximal femoral morphology [8-11,18,25]. Lutz et al found that medial calcar attenuation was lower among Dorr Type C femora, although their study used a more localized ROI [18]. Bukowski et al demonstrated that CT scans obtained for robotic-assisted THA could identify previously unrecognized osteoporosis and potentially influence fixation planning but did not specifically characterize the stepwise relationship between multi-site HU and Dorr classification [14]. The current study extends this literature by evaluating a comparatively large robotic THA cohort and directly comparing an isolated femoral neck measurement with a three-site composite measure.

Performance of Composite Versus Femoral Neck HU

Composite average HU demonstrated a stronger correlation with ordinal Dorr classification and greater discrimination of Dorr Type C morphology than femoral neck HU alone. This difference may partly reflect the limitations of relying on a single anatomic measurement. Femoral neck HU can be affected by ROI placement, local cortical inclusion, femoral positioning, degenerative change, and imaging artifact [23,24]. Averaging measurements obtained from L4, FN, and IT may reduce the influence of localized variation and provide a more stable estimate of overall skeletal attenuation. The composite measure may capture systemic skeletal attenuation in addition to local proximal femoral characteristics. This distinction is important because Dorr classification primarily describes femoral morphology, whereas HU quantifies radiographic attenuation and may reflect both local anatomy and generalized bone quality. The two measures therefore provide related but not identical information.

The multivariable findings further supported the performance of the composite measure. Each 10-HU decrease in composite average HU was associated with 43% greater odds of belonging to a higher Dorr category after adjustment for age, sex, and BMI. Composite HU also provided better model fit than femoral neck HU in the binary analysis of Dorr Type C versus Type A or B morphology. Although modeling HU continuously preserved more information and produced superior statistical fit, the dichotomized composite threshold retained clinically useful discrimination. These findings favor reporting composite HU as a continuous measure while reserving threshold values for screening and clinical interpretation rather than treating them as definitive diagnostic categories.

Interpretation of the HU Thresholds

ROC analysis and regression models translated the HU-Dorr relationship into clinically interpretable parameters (Table 3; Figure 2) with average composite HU outperforming femoral neck HU across statistical frameworks, identifying 83 of 101 Dorr C patients (82.2% sensitivity) at ≤117.6 HU, compared with 63 of 101 (62.4% sensitivity) for femoral neck cutoff HU of ≤87. These thresholds are biologically plausible and consistent with other studies. Hoyt et al demonstrated strong correlations between femoral neck HU and DEXA-derived bone mineral density and reported femoral neck thresholds of approximately 151 HU for low bone mineral density and 98 HU for osteoporosis [25].

The ≤117.6 HU threshold should be interpreted as a screening threshold, not a universal diagnostic cutoff because optimal HU values vary with scanner protocol, ROI, population, and reference standard [10,12,26]. In practice, low average HU combined with Dorr C morphology reinforces concern for poor bone quality and may prompt closer radiographic review, metabolic bone evaluation, or heightened intraoperative caution, whereas discordant HU and Dorr findings should prompt reassessment of classification and consideration of additional evaluation.

Periprosthetic Risk Stratification

While the low periprosthetic fracture incidence (n = 6) precludes multi-variable hazard modeling, all fractures occurred in the concordant low-HU/Dorr C cohort suggesting a strong negative predictive value screening signal. Notably, HU seemed to stratify risk even within the Dorr C cohort with the 30 Dorr C patients with preserved femoral neck HU (≥87) experiencing no fractures, implying that HU-based bone quality assessment could identify Dorr C patients in whom cementless press-fit stems remain reasonable, rather than choosing a cemented stem based on Dorr type alone. Although exploratory, this aligns with literature linking Dorr C morphology to increased fracture risk [6,7,26]. This suggests that HU triage could help flag patients requiring primary cemented fixation or alternative stem selection without adding diagnostic overhead [6,7,22]. Future studies should evaluate whether HU-informed preoperative planning alters implant selection and reduces fracture incidence.

Clinical Utility

The most practical advantage of this study is its integration into an existing robotic workflow that often relies on preoperative CT for planning, implant sizing, and component positioning [12,13]. In most institutions, attenuation data is generated automatically but not routinely reported [14]. Our findings support an addition to that workflow: extracting HU values that are already present and using them to objectify bone quality assessment before surgery. This would be easy for the radiologist and add objective data to implant selection.

A recent review of 58 studies concluded that HU can be used preoperatively to assess hip bone quality, guide surgical approach, predict intraoperative fracture, and inform perioperative decision-making [27]. Our results extend that literature by defining how HU relates specifically to Dorr morphology in a large cohort and by identifying a composite average HU measure that outperforms single-site femoral neck HU.

In practice, HU-based screening within the robotic planning environment may support several preoperative actions without additional imaging, cost, or radiation:

1. Preoperative triage: Patients with average HU ≤117.6 and/or radiographic Dorr C may be flagged for enhanced counseling regarding fracture risk, bone health optimization, and strategy.
2. Fixation planning: Objective low HU may lower the threshold to consider cemented femoral fixation, alternative stem geometry, or more cautious canal preparation, particularly when Dorr typing is equivocal [6,14,22].
3. Workflow standardization: Incorporating HU into the preoperative checklist may reduce reliance on subjective radiographic interpretation and improve generalizability [5].
4. Opportunistic metabolic bone assessment: Patients with unexpectedly low HU may be referred for osteoporosis management [14,25].

This creates opportunity to repurpose data that is currently acquired for navigation, into a standardized bone-quality readout during surgical planning.

Although this study did not include sufficient fracture events for outcome-based modeling, Dorr classification remains clinically relevant because it reflects proximal femoral geometry and bone quality that influence operative and post-operative planning. The value of CT-derived HU is not to replace Dorr classification, but to provide an objective, workflow-integrated measure that corroborates radiographic typing before implant selection.

Limitations

This study has several limitations. Its retrospective, single-health-system design may introduce selection bias and limit generalizability to institutions with different populations, CT protocols, scanners, or surgical practices. HU measurements may also vary with scanner calibration, reconstruction parameters, image artifacts, intra-observer and inter-observer variability, and ROI placement. We did not correlate HU with DEXA T-scores, which would strengthen interpretability [25]. Finally, the proposed average HU cutoff

is a derivation-set screening threshold and requires confirmation in independent cohorts. Finally, only six periprosthetic fractures occurred, precluding multivariable outcome modeling and limiting adjustment for implant design, fixation strategy, surgical approach, surgeon technique, and other confounders; therefore, the fracture findings should be considered exploratory and should not be used to establish treatment or fixation thresholds.

Future Directions

Future studies should externally validate the composite HU threshold in independent cohorts. Direct comparison with DEXA would help determine whether composite HU primarily reflects systemic bone density, local proximal femoral morphology, or both. Formal inter-observer and intra-observer reliability testing is needed, and automated or semiautomated HU extraction may improve reproducibility and facilitate integration into preoperative planning software [28]. Most importantly, larger outcome-focused studies should determine whether HU adds predictive value beyond Dorr classification.

Conclusion

In patients undergoing CT-planned robotic-assisted primary THA, CT-derived HU demonstrated a strong, stepwise association with radiographic Dorr classification. A composite measure incorporating L4, FN, and IT attenuation outperformed isolated femoral neck HU for identifying Dorr Type C morphology, with a cohort-derived screening threshold of ≤117.6 HU. Because these measurements can be obtained from CT imaging already acquired for robotic planning, HU provides an objective, workflow-integrated adjunct when radiographic Dorr classification is equivocal. However, the proposed threshold requires external validation, and the exploratory fracture findings are insufficient to support fixation or treatment decisions. HU should therefore complement, rather than replace, radiographic assessment, clinical judgment, and intraoperative evaluation.

Declarations

Ethics approval and consent to participate

SLH IRB exemption: SLHS-24-076

Consent for publication

Not applicable.

Availability of data and materials

Deidentified data may be available from the corresponding author upon reasonable request and with approval from the Saint Luke's Health System and applicable institutional review board requirements.

Conflict of Interest

The authors have no conflicts of interest to declare.

Funding Sources

This study was not supported by any sponsor or funder.

Author Contributions

ZM assisted with Conceptualization, Methodology, Data Curation, Investigation, Validation, Writing - Original Draft & Review & Editing.; RM assisted with Conceptualization, Methodology, Data Curation, Investigation, Validation, Formal Analysis, Writing - Original Draft & Review & Editing.; FB assisted with Conceptualization, Formal Analysis, Writing - Original Draft & Review & Editing; SM assisted with Conceptualization, Data Curation, Writing - Review & Editing; AK assisted with Data Curation, Investigation, Resources (Data Acquisition), Writing - Review & Editing, and Supervision; JWK assisted with Project Administration, Conceptualization, Resources (Data Acquisition), Writing - Review & Editing, and Supervision.

References

1. Sloan M, Premkumar A, Sheth NP (2018) Projected Volume of Primary Total Joint Arthroplasty in the U.S., 2014 to 2030. J Bone Joint Surg Am 100(17):1455–1460. 10.2106/JBJS.17.01617
2. Kurtz S, Ong K, Lau E, Mowat F, Halpern M (2007) Projections of primary and revision hip and knee arthroplasty in the United States from 2005 to 2030. J Bone Joint Surg Am 89(4):780–785. 10.2106/JBJS.F.00222
3. Dorr LD, Faugere MC, Mackel AM, Gruen TA, Bognar B, Malluche HH (1993) Structural and cellular assessment of bone quality of proximal femur. Bone 14(3):231–242. 10.1016/8756-3282(93)90146-2
4. Nash W, Harris A (2014) The Dorr Type and Cortical Thickness Index of the Proximal Femur for Predicting Peri-Operative Complications during Hemiarthroplasty. J Orthop Surg 22(1):92–95. 10.1177/230949901402200123
5. Nakaya R et al (2019) Reproducibility of the Dorr classification and its quantitative indices on plain radiographs. Orthop Traumatol Surg Res 105(1):17–21. 10.1016/j.otsr.2018.11.008
6. Gromov K, Bersang A, Nielsen CS, Kallemose T, Husted H, Troelsen A (2017) Risk factors for post-operative periprosthetic fractures following primary total hip arthroplasty with a proximally coated double-tapered cementless femoral component. Bone Jt J 99–B(4):451–457. 10.1302/0301-620X.99B4.BJJ-2016-0266.R2
7. Zhao WQ, Yu KQ, Xie RZ, Liang YF, Huang JF (2025) Risk factors for periprosthetic femoral fractures following hip arthroplasty: a systematic review and meta-analysis. Ann Med 57(1):2494679. 10.1080/07853890.2025.2494679
8. Pickhardt PJ, Pooler BD, Lauder T, del Rio AM, Bruce RJ, Binkley N (2013) Opportunistic screening for osteoporosis using abdominal computed tomography scans obtained for other indications. Ann

Intern Med 158(8):588–595. 10.7326/0003-4819-158-8-201304160-00003

9. Schreiber JJ, Anderson PA, Rosas HG, Buchholz AL, Au AG (2011) Hounsfield units for assessing bone mineral density and strength: a tool for osteoporosis management. J Bone Joint Surg Am 93(11):1057–1063. 10.2106/JBJS.J.00160
10. Andresen JR, Schröder G, Haider T, Schober HC, Andresen R (2025) Osteoporosis Assessment Using Bone Density Measurement in Hounsfield Units in the Femoral Native CT Cross-Section: A Comparison with Computed Tomography X-Ray Absorptiometry of the Hip. Diagnostics 15(8):1014. 10.3390/diagnostics15081014
11. Opportunistic CT- (2026) based osteoporosis screening of the hip: a systematic review of diagnostic accuracy | Archives of Orthopaedic and Trauma Surgery | Springer Nature Link. Accessed June 24. https://link.springer.com/article/10.1007/s00402-025-06130-1
12. Perazzini P, Trevisan M, Sembenini P et al (2020) The Mako™ robotic arm-assisted total hip arthroplasty using direct anterior approach: surgical technique, skills and pitfalls. Acta Bio Med Atenei Parm 91(4–S):21–30. 10.23750/abm.v91i4-S.9659
13. Wan L, Lee CY, Park KS (2026) MAKO Robotic-Arm-Assisted Versus Conventional Dual-Incision Total Hip Arthroplasty: A Propensity-Score-Matched Retrospective Study. J Clin Med 15(2):405. 10.3390/jcm15020405
14. Bukowski BR, Sandhu KP, Bernatz JT et al (2023) CT required to perform robotic-assisted total hip arthroplasty can identify previously undiagnosed osteoporosis and guide femoral fixation strategy. Bone Jt J 105–B(3):254–260. 10.1302/0301-620X.105B3.BJJ-2022-0870.R1
15. Li J, Zhang M, Yao J, Shao L, Fang C, Cheng CK (2024) Risk Factors for Periprosthetic Femoral Fractures After Cementless Total Hip Arthroplasty. J Arthroplasty 39(10):2547–2554. 10.1016/j.arth.2024.06.005
16. Primary total hip arthroplasty using a short bone-conserving stem in young adult osteoporotic patients with Dorr type C femoral bone | Journal of Orthopaedic Surgery and Research | Springer Nature Link. Accessed June 24 (2026) https://link.springer.com/article/10.1186/s13018-020-01985-z
17. Wilkerson J, Fernando ND (2020) Classifications in Brief: The Dorr Classification of Femoral Bone. Clin Orthop 478(8):1939–1944. 10.1097/CORR.0000000000001295
18. Lutz RW, Thalody H, Alexander T et al Medial Calcar Density Measured via Opportunistic Computed Tomography Is Well Represented by the Dorr C Classification. Cureus. 16(6):e62428. 10.7759/cureus.62428
19. Lim HK, Ha HI, Park SY, Lee K (2019) Comparison of the diagnostic performance of CT Hounsfield unit histogram analysis and dual-energy X-ray absorptiometry in predicting osteoporosis of the femur. Eur Radiol 29(4):1831–1840. 10.1007/s00330-018-5728-0
20. Kim YS, Lee S, Sung YK, Lee BG (2016) Assessment of osteoporosis using pelvic diagnostic computed tomography. J Bone Min Metab 34(4):457–463. 10.1007/s00774-015-0684-0

21. Lee BJ, Koo HW, Yoon SW, Sohn MJ (2021) Usefulness of Trabecular CT Attenuation Measurement of Lumbar Spine in Predicting Osteoporotic Compression Fracture: Is the L4 Trabecular Region of Interest Most Relevant? Spine 46(3):175–183. 10.1097/BRS.0000000000003756
22. Kheir MM, Dilley JE, Speybroeck J et al (2023) The Influence of Dorr Type and Femoral Fixation on Outcomes Following Total Hip Arthroplasty for Acute Femoral Neck Fractures: A Multicenter Study. J Arthroplasty 38(4):719–725. 10.1016/j.arth.2022.10.028
23. Jang S, Graffy PM, Ziemlewicz TJ, Lee SJ, Summers RM, Pickhardt PJ (2019) Opportunistic Osteoporosis Screening at Routine Abdominal and Thoracic CT: Normative L1 Trabecular Attenuation Values in More than 20 000 Adults. Radiology 291(2):360–367. 10.1148/radiol.2019181648
24. Zhou F, Zhang W, Geng J et al (2024) Comparisons of Hounsfield units and volumetric bone density in discriminating vertebral fractures on lumbar CT scans. Br J Radiol 97(1157):1003–1009. 10.1093/bjr/tqae053
25. Femoral Neck Hounsfield Units as an Adjunct for Bone Mineral Density After Combat-Related Lower Extremity Amputation. - Abstract - Europe PMC. Accessed June 24 (2026) https://europepmc.org/article/med/33079846
26. Abdel MP, Watts CD, Houdek MT, Lewallen DG, Berry DJ (2016) Epidemiology of periprosthetic fracture of the femur in 32 644 primary total hip arthroplasties: a 40-year experience. Bone Jt J 98–B(4):461–467. 10.1302/0301-620X.98B4.37201
27. CT Hounsfield units in assessing bone and soft tissue quality in the proximal femur: A systematic review focusing on osteonecrosis and total hip arthroplasty | PLOS One. Accessed June 24 (2026) https://journals.plos.org/plosone/article?id=10.1371/journal.pone.0319907
28. Khanuja HS, Mekkawy KL, MacMahon A, McDaniel CM, Allen DA, Moskal JT (2022) Revisiting Cemented Femoral Fixation in Hip Arthroplasty. J Bone Joint Surg Am 104(11):1024–1033. 10.2106/JBJS.21.00853

Figures

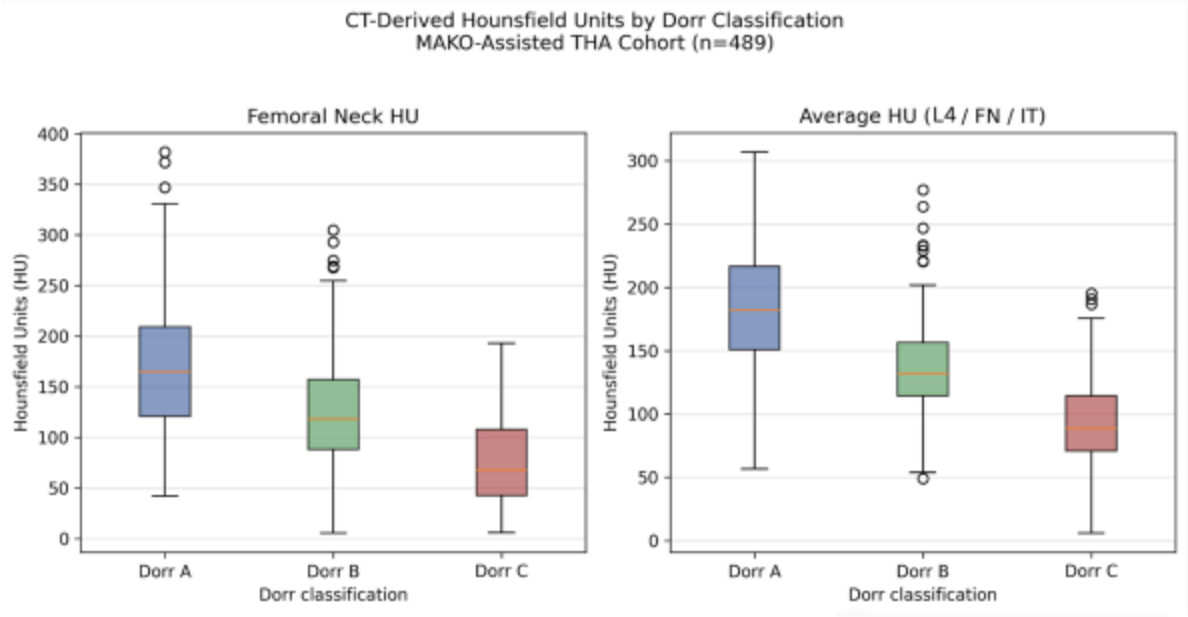


Figure 1

Legend not included with this version.

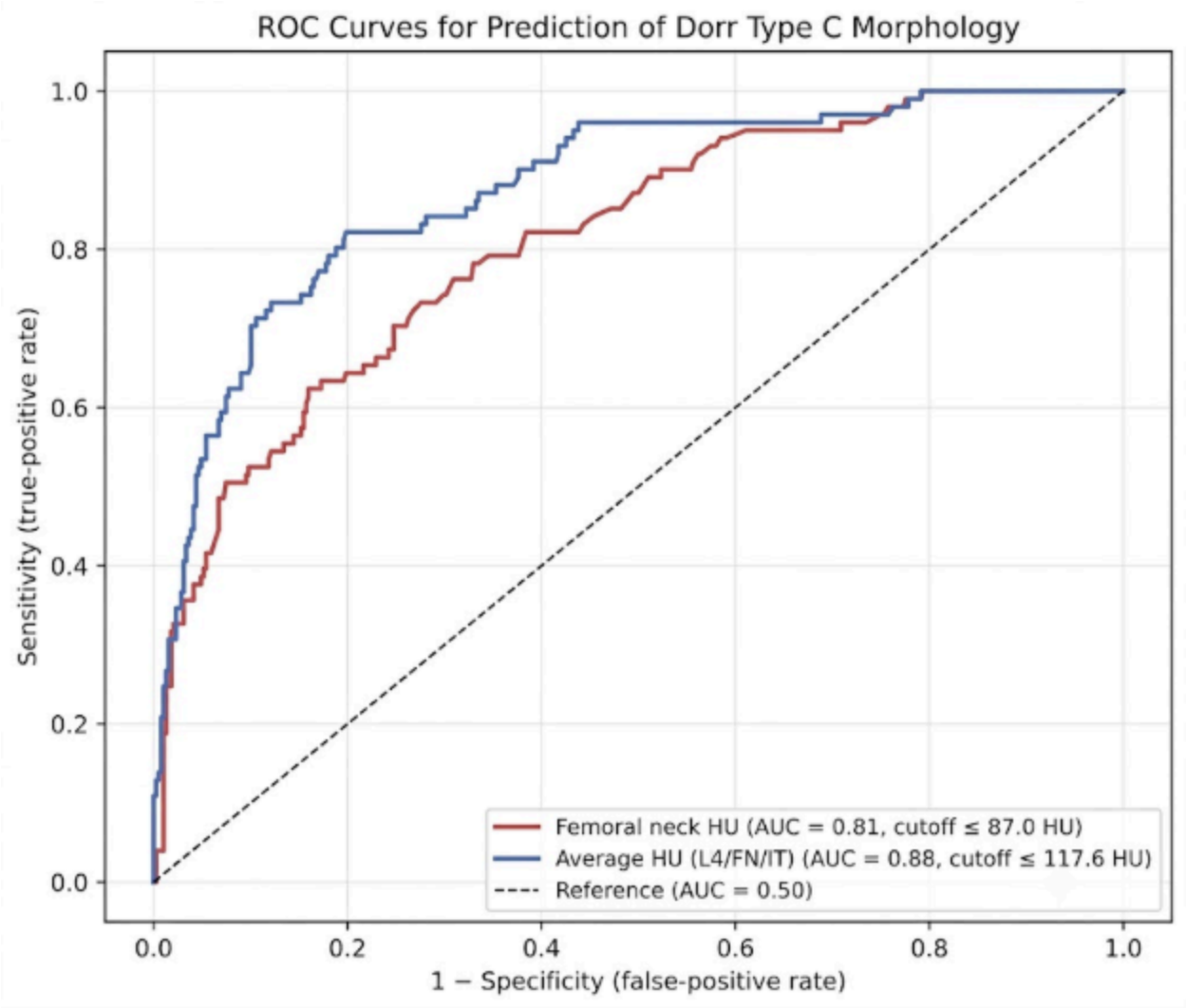


Figure 2

Legend not included with this version.

Supplementary Files

This is a list of supplementary files associated with this preprint. Click to download.

- MAKOCleanSheet1.pdf